RESEARCH PAPER

Test Setup for Investigating the Impact Behavior of Biaxially Prestressed Composite Laminates

C. Pongratz[1] · J. Tix[2] · J. Wolfrum[3] · S. Gerke[2] · I. Ehrlich[1] · M. Brünig[2]

Abstract

Instrumented impact testing and compression-after-impact testing are important to adequately qualify material behavior and safely design composite structures. However, the stresses to which fiber-reinforced plastic components are typically subjected in practice are not considered in the impact test methods recommended in guidelines or standards. In this paper, a test setup for investigating the impact behavior of composite specimens under plane uniaxial and biaxial preloading is presented. For this purpose, a special test setup consisting of a biaxial testing machine and a specially designed drop-weight tower was developed. The design decisions were derived from existing guidelines and standards with the aim of inducing barely visible impact damage in laminated carbon fiber-reinforced plastic specimens. Several measurement systems have been integrated into the setup to allow comprehensive observation of the impact event and specimen behavior. A feasibility test was performed with biaxially prestressed carbon fiber-reinforced plastic specimens in comparison with unstressed reference tests. The compressive-tensile prestressing resulted in lower maximum contact forces, higher maximum deflections, higher residual deflections and a different damage pattern, which was investigated by light microscopic analysis. Finally, the functionality of the experimental setup is discussed, and the results seem to indicate that the test setup and parameters were properly chosen to investigate the effect of prestresses on the impacts behavior of composite structures, in particular for barely visible subsequent damages.

✉ C. Pongratz
christian1.pongratz@oth-regensburg.de

✉ I. Ehrlich
ingo.ehrlich@oth-regensburg.de

J. Tix
janek.tix@unibw.de

J. Wolfrum
johanneswolfrum@bundeswehr.org

S. Gerke
steffen.gerke@unibw.de

M. Brünig
michael.bruenig@unibw.de

[1] Labor Faserverbundtechnik, OTH Regensburg, Galgenbergstraße 30, 93053 Regensburg, Germany

[2] Institut für Mechanik und Statik, Universität der Bundeswehr München, Werner-Heisenberg-Weg 39, 85579 Neubiberg, Germany

[3] Wehrwissenschaftliche Institut für Werk- und Betriebsstoffe, Institutsweg 1, 85435 Erding, Germany

Introduction

The main advantage of fiber-reinforced plastics is the excellent ratio of stiffness and strength compared to their material density. The high specific stiffness and strength composites offer are useful in many applications concerned with efficiency or mass reduction. In addition, composites possess quite diverse properties and characteristics depending on the fiber reinforcement and matrix type, laminate structure and manufacturing process, thus making them attractive for many specialized applications. However, each material has its own weaknesses that must be taken into account when applying the material and designing structures with it. In the case of fiber-reinforced plastics, their rather brittle behavior is often a concern.

In combination with impact loads, this material behavior can lead to complex material degradation in fiber-reinforced plastic structures. In the case of so-called low-velocity impacts (LVI), such damages can be particularly dangerous as they are often not or only barely visible from the outside.

This category of damage is often referred to as so-called barely visible impact damage (BVID) and causes risks due to wide areal cracks, i.e. delaminations within the laminate structure. Delaminations can significantly reduce the compression strength and the fatigue behavior of the laminate. The effect of impacts is a well-known issue in the application of fiber-reinforced plastics and demonstrates why tensile and compression tests alone are not sufficient for qualifying composite materials. Instrumented impact tests and post-impact compression tests are also required to adequately predict material behavior. Different investigations have shown that in-plane prestressing has an effect on the impact behavior of fiber-reinforced plastics, which are generally present during the use of mechanical components.

In order to understand and describe the influence of in-plane biaxial prestresses on the impact behavior of fiber-reinforced plastics, a test setup was developed. A biaxial testing machine was chosen for the test setup, which allows combined tensile and compressive loading of cross-shaped specimens. In addition, an adapted test tower was developed and integrated into the biaxial testing machine. The following sections outline the test methodology, data setup and processing, and describe a final feasibility test comparing specimens prestressed by a biaxial load condition with unloaded reference tests.

Overview on Impact Testing with Prestresses

Impact testing of composites is performed differently depending on the examination task and research topic. In most cases, the impact velocity and impact energy, the size and material of the specimen, and the installation conditions with boundary restrictions and free area sizes represent important impact variables. Some uniformity in approach is provided by standards and specific guidelines, often related to the aviation industry and its safety-oriented design approach, i.e., the damage-tolerant design strategy. Many researchers and investigators use broadly similar impact test setups that are most likely derived from, or at least guided by, these recommendations, allowing for some comparability of results and findings.

In the following, the most important guidelines and standards for impact testing are briefly presented, followed by the approaches of researchers investigating the effect of prestressing on the impact behavior. Finally, an impression of the current state of the art on investigating biaxially prestressed specimen and its main results is described.

Guidelines and Standards

Evaluation methods for estimating the damage severity for low-velocity impacts are now largely standardized. While the first setup recommendations for impact testing were most likely derived from Charpy-like test setups, i.e., as described in the American Society for Testing and Materials' Selected Technical Paper STP 563 (1973), the first guideline using today's common procedure with larger test structures and the subsequent residual compressive strength testing was probably NASA's Reference Paper RP 1092, published in the early 1980s. Following these publications, other aviation actors such as the Royal Aerospace Establishment with its Composite Research Advisory Group and The Boeing Company, published the CRAG Method 403 and Boeing Specification Support Standard BSS 7260 respectively, with Airbus S.A.S. issuing the Airbus Test Method AITM-0010 in 1994.

The aviation industry guidelines were joined in subsequent years by institutional standards such as the DIN 65561 of the German Institute for Standardization, the SACMA Recommended Method SRM 2R of the Suppliers of Advanced Composite Materials Association or the JIS K 7089 of the Japanese Standards Association. Since then, the DIN 65561 has been replaced by DIN EN 6038 and, together with the ISO 18352 and the ASTM D7136, represents probably some of the most common international standards for impact and residual compressive strength testing.

Standards and guidelines vary in their specifications, but most approaches recommend a similar design and test procedure. Impact tests are performed with a drop-weight tower and a fixture consisting of a rectangular free window within a support frame. For impact induction, the specimens are placed on the support frame and fixed with quick-release levers, a bolted frame, or similar methods. After clamping, the impact mass is released from a set height, stopped after initial contact and rebound, and reset. After being damaged by the impact, the specimen is placed in a guiding device and compressively loaded until failure occurs.

Specimen for impact testing are generally thin rectangular plates with dimensions of 150 mm x 100 mm x 4 mm, while the free window size is in the range of 125 mm x 75 mm. The recommended stacking order for the laminate differs for fabric-type and unidirectional single layers, but mostly symmetrical quasi-isotropic laminates of $[[+45°/0°/-45°/90°]_n]_s$ are used with varying sublaminate repeats n to achieve an overall laminate thickness ideally close to the aforementioned 4 mm. The impactor used in most experimental setups has a spherical metal tip of approximately 16 mm diameter. There are major differ-

ences in impactor mass and drop height recommendations both between and within the guidelines and standards. Nevertheless, the most common impactor masses for low-velocity impact testing are probably in the range of 1 to 7 kg.

Investigation Approach in Research Studies

When the influence of prestresses on the impact behavior of structures became apparent, several research groups developed experimental setups to study these effects. While most studies are similar in that a loading condition is first established for the test structures and then the impact test is performed, the stress and strain state investigated varies depending on the objectives of the different research studies. Most of the works found deal with torsion, bending, or plane uniaxial and biaxial stressed structures, the latter also being the focus of this work.

Following analytical studies and Charpy-like experimental tests with uniaxially prestressed composite beams in the late 1970s and 1980s, experimental studies with setups similar to today's guidelines and standards became available in the work of Sankar & Sun [1] on the subject of uniaxially tensile prestressed carbon fiber-reinforced plastic (CFRP) sheets in 1985, while Morlo & Kunz [2] and Nettles & Lance [3] followed up in the early 1990s with studies on uniaxially compression prestressed CFRP.

While Sankar & Sun [1] used two clamps and a pneumatic cylinder to apply the prestress and an air propelled impactor delivery, Morlo & Kunz [4] placed the specimens in a clamping frame and applied the compressive preload in a universal testing machine. After freezing the stresses in the specimen by wedged screw joining the plates to the frame, the fixture could be placed in a drop-weight tower and tested in a more conventional manner. Nettles & Lance [3] used a specially developed preloading device that can be installed completely under a standard impact testing machine. The preloading device essentially consists of two steel plates and a hydraulic cylinder to apply the compressive preloads prior to the impact. In a later investigation in 1995, Nettles et al. [5] also conducted tests using a modified preloading device for uniaxial tension prestressing. In the papers, the preload-dependent contact force histories as well as the residual compressive strength values were presented as results. Sankar & Sun [1] also presented initial ultrasonic scans, while Morlo & Kunz [2, 4] also additionally measured the impactor displacement and calculated energy-time curves.

In the following years, further important studies have dealt with the influence of uniaxial tensile and compressive prestressing on the impact behavior at low [6–10] and high velocities [11–13], in some cases presenting different test setups. In particular, however, the development and design of test setups for impact tests under biaxial prestresses should be highlighted as an important advance. Such investigations

were conducted by a research group connected by Marshall I.H. with publications from Robb et al. [14], Whittingham et al. [15] and Mitrevski et al. [16] between 1995 and 2006, by García-Castillo et al. in 2007 [17], Garnier et al. in 2011 [18], as well as by Kurşun & Şenel in 2011 [19] and 2015 [20], respectively.

Similarly to uniaxial setups, testing with biaxial preloads also starts by establishing a preload condition and subsequently performing the impact test. While Garnier et al. [18] and García-Castillo et al. [17] extended existing vertically built biaxial testing machines with an impact pendulum and a gas gun, respectively, the other mentioned works used specially designed setups of horizontal biaxial loading devices in combination with drop-weight towers, very similar to the uniaxial approach of Nettles & Lance [3]. In these cases, the loading fixtures were L-shaped, with two perpendicular pneumatic cylinders for load application and two fixtures on the other side of the specimen. The specimens were usually thin rectangular or square shapes, sometimes with metal tabs near the edges for load introduction. In the publications based on work with biaxial testing machines, cross-shaped geometries with large central areas were chosen instead of square shapes.

Excluding the gas gun setup for high velocity testing, most of the tests were conducted in a test range with impact energies from 4 to 24 J and preloads of 2 to about 20 kN, which in most cases corresponds to prestrains of approximately 500 to 6000 μm/m, depending on the material type and specimen dimensions. In addition to the impact energy, it should be noted that the impactor tips mentioned in the papers often possess a diameter of 10 to 12 mm, and are thus somewhat smaller compared to most standards and guideline recommendations.

Results on the Impact Behavior with Biaxial Prestressing

The investigation results of the impact behavior of biaxially prestressed composites differ between the works, which can be mainly attributed to the different materials, preload levels and impact parameters. Most works presented data on glass-fiber reinforced plastic (GFRP) specimen [14, 16, 17, 19, 20] while results on the impact behavior of CFRP speicmen [15, 18] were less common. In almost all investigations, the force-time histories obtained provided an important basis for deriving effects and assessing the influence of preloads. Results on the residual compressive after impact (CAI) strength were not presented, though Garnier et al. [18] were planning rectangular specimen cutouts for possible future compression testing. Instead, data on the dissipated energy during the impact event and indentation depth values were often used as assessments of the damage severity.

SEM

Especially the investigations of Robb et al. [14] and Whittingham et al. [15] presented comprehensive experimental studies on the effect of biaxial prestresses, with the first focusing on chopped-fiber GFRP and the latter on CFRP specimen. While Robb et al. [14] concluded that impact behavior of GFRP sheets is strongly dependent upon the nature of prestress and observed the maximum damage level for a tension-compression condition, Whittingham et al. [15] concluded for the CFRP sheets tested, that the prestresses within their study parameters with near penetration failure had no significant effect on the measured peak force and absorbed energy values.

Experimental Setup

The developed test setup, presented in this paper, is based on an existing biaxial preload testing machine and was designed for impact testing of cross-shaped structures under plane uniaxial and biaxial prestresses. The setup consists of a specially developed drop-weight tower that can be installed on the biaxial testing machine. A picture of the overall test setup with image impressions of the different test elements and measurement systems can be seen in Fig. 1.

Figure 1 (a) illustrates the location of the measurement systems and main components that are either integrated into the drop-weight tower system or set up after the tower is installed onto the biaxial testing machine. One main component of the drop-weight tower is the weight itself, which is equipped with a load cell between the impact mass and the tip of the impactor (g) and a laser reflector on the left side of the impact mass (b). A light barrier flag is attached to the right side of the mass, which automatically triggers the start of several measuring systems as soon as the light barrier signal is interrupted by the flag (h). The laser distance sensor aimed at the attached reflector is mounted at the base of the drop-weight tower (d). A second laser distance sensor is mounted on a hinge on the base plate of the biaxial testing machine along with two high-speed cameras (k) and three cameras of a digital image correlation system (f). The second laser system and the cameras are directed at the lower surface of the installed specimen (e). The biaxial testing machine has four clamping elements for load application (j). Before the test, two acoustic emission sensors are attached to the specimen in the outer areas of the impact zone (c). After the impact event, two automatically extending catcher elements stop the impactor (i), thus preventing unwanted secondary damages. The main components and measuring systems are described in more detail in the following sections.

Biaxial Testing Machine

The key element in the test setup is the biaxial testing machine LFM-BIAX 20 kN, manufactured by Walter+Bay, Switzerland, see Fig. 1 (a). The four electromechanically driven cylinders can be individually force or displacement controlled and have a maximum load capacity of 20 kN (tension and compression). The machine control described in "Prestress Application" is implemented using the Dion7 software provided with the machine. The working area is arranged horizontally and thus in generally allows the use of a vertical impactor on the loaded specimen, although this type of impact loading was not envisaged when the machine was designed by Walter+Bai. The main field of application of the machine is the testing of newly developed biaxial flat specimens made of ductile metal under proportional and non-proportional loading, see e.g. [21, 22]. Consequently, care must be taken in the design of the other test equipment to ensure that no excessive impact loads, especially not transverse to the axes, act on the cylinders.

In its normal application, the biaxial machine is operated with a double-sided image correlation system. This is possible due to the fact that the solid base plate has a circular opening below the test area. As the impactor is positioned from above, optical measurement from above is not possible in the planned series of experiments. However, the underside of the specimen can be approached, as long as the vertical specimen supports leave this area sufficiently free. Furthermore, the maximum specimen size is determined by the installation space. With the current machine setting, this is 300 mm x 300 mm. Consequently, these basic requirements of the biaxial machine must be met with the newly designed test equipment and test specimens described hereafter.

Specimen Design

The specimens were designed as axisymmetric thin cross-shaped plates with a large circular area in the center for impact testing and four protruding sections for load introduction as shown in Fig. 2. Initial considerations for deriving a suitable specimen shape are based on preliminary works with the biaxial testing machine and experience on the load application to metallic specimens [21, 22]. The shape of test specimen is intended to ensure a strain state as homogeneous as possible for different load types in the impact area. Also, there is no for need metallic tabs for load introduction or composite non-appropriate cuts and cutouts. Although various materials and layer structures are conceivable for the investigations, the development of the setup focused on car-
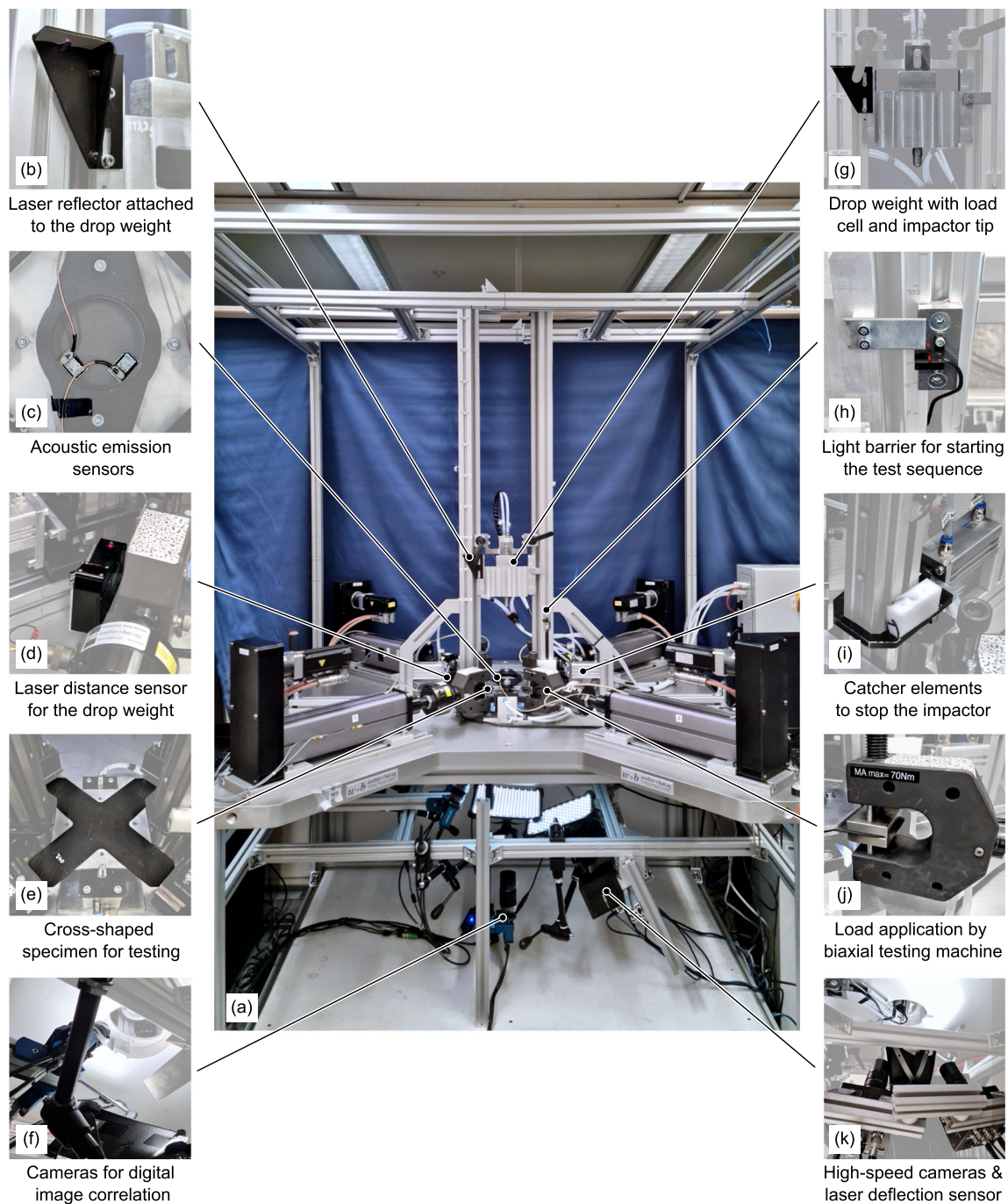
Fig. 1 Developed test setup for investigating the impact behavior under uniaxial and biaxial prestresses (a) including main components and measurement systems (b–k)

bon fiber-reinforced plastic and the material and mechanical properties that can be expected with it.

Several aspects were considered when dimensioning the specimens: First, in order to achieve comparability with other investigations and studies, dimensions close to the guidelines and standard recommendations for specimen sizes in the range of 150 mm x 100 mm seem to be reasonable. Second, the loading capacity of the biaxial testing machine is

limited, so smaller sizes allow the investigation of higher stresses and strains. However, this is countered by the third consideration that the boundary conditions and the frame of the fixture approach the impact area and change the behavior of the specimen, which is not desirable. Weighing these considerations, the dimensions of 290 mm x 290 mm were chosen for the total specimen size, slightly smaller than the maximum insert sizes of the biaxial testing machine for top
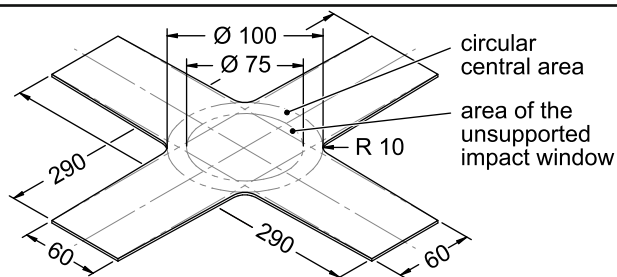
Fig. 2 Dimensions of the specimen in mm with indication of the construction lines and the central test area

loading. The central area of the specimen was set to a diameter of 100 mm. The protruding sections follows the 60 mm width of the clamping jaws of the biaxial testing machine. For the transition between the protruding sections and the central area, a tangential transition with a radius of 10 mm was selected. Although various specimen thicknesses are conceivable, considering the maximum load capacity of the biaxial testing machine as well as the magnitude of realistic preloads and impact conditions for CFPR, thicknesses from 1 to 4 mm fall within the scope of reasonable test cases.

Support Fixture

A carrier and pressure frame with a circular impact window were selected to match the inner circular specimen area which can be seen in Fig. 3. After the prestress condition is reached, the clamping frame is pressed onto the specimen by two Festo compact pneumatic cylinders of type ADN-50-20-A-P-A with a gauge pressure of 4.8 bar. The diameter of the free area is 75 mm, which is based on the shorter projection length from many standard and guideline recommendations. After initial preliminary tests with prestresses, the mounting area was supplemented by additional metal guides above and below the specimen. These minimize the unsupported free lengths and reduce the risk of stability failure during tests with a compression component. The upper guide plate can be set via four screws and tests were carried out to determine a suitable torque that locks the frame without play and without hindering the formation of deformations in the middle area of the specimen. Furthermore, the alignment between the guiding plates and the clamping jaws of the biaxial testing machine was set quite carefully, as non-planar deformations might be caused by misalignment.

Prestress Application

The prestressing of the specimen is realized by the biaxial testing machine described above. Figure 4 shows a schematic representation with an inserted specimen as well as the axis designation. To keep the application of the preload as symmetrical as possible, a predominantly displacement-
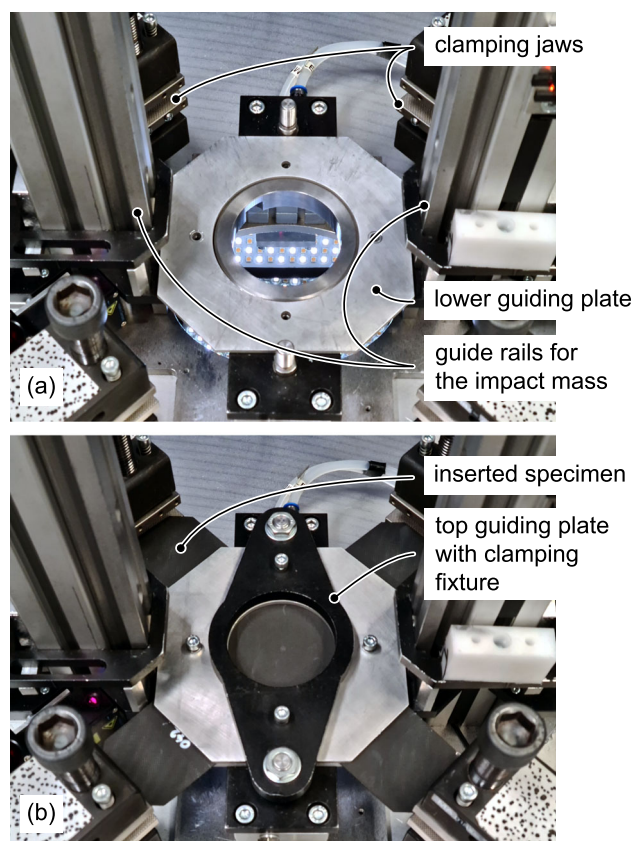

Fig. 3 Circular support before insertion of the specimen (a) and after installation (b)

controlled test routine is used. Simultaneously the cylinders are controlled as follows:

- The machine displacement u_{C1} of cylinder $C1$ (leading) is continuously increased by 0.04 mm/min.
- The same displacement is applied on the cylinder $C3$ on the opposite side of the same axis ($A1$) as u_{C3}.
- The generated force F_{C1} is taken, multiplied by the load factor and applied on the cylinder $C2$ as F_{C2} in axis 2 ($A2$). This causes the machine displacement u_{C2} while only this cylinder $C2$ is force driven.
- On cylinder $C4$ (opposite side of $A2$) the same displacement is applied, i.e. $u_{C4} = u_{C2}$.

Whereby the notation and axis designations from Fig. 4 are used and cylinders 1 to 4 are labeled C1 to C4 and axes 1 and 2 are identified as A1 and A2. Furthermore, after reaching the preload level, all cylinders are set to hold. Thus, the preload remains symmetrical with respect to the displacements and small deviations in the forces must be accepted. The biaxial preloads are to be applied with a fixed load ratio in the two axes. In practical implementation, however, small deviations in the loads of the cylinders of one axis can hardly be avoided. These can be caused, among other things,
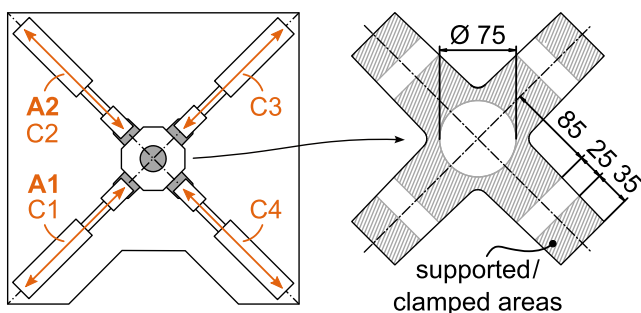
Fig. 4 Axis designation of the biaxial testing machine and clamping areas of the specimen with dimensions in mm

by slightly asymmetrical specimens, small deviations in the machine alignment or effects from the specimen clamping. In the present test sequence, after insertion and clamping of the specimens, the cylinders are driven until the individual forces are again at zero in order to partially compensate for such effects.

The test specimen is clamped as described here: After inserting the specimen, the clamping jaws are brought into position and moved towards the support fixture. The clamping jaws are mechanically set via a screw which is tightened to 70 Nm using a torque wrench. The clamping jaws are fitted with a groove pattern that leaves impressions in the protruding parts of the specimen. However, since the force is applied at a sufficient distance from the impact area, unintended influences on the impact behavior seem unlikely, while it offers the advantage of good force transmission and eliminates the need for additional bolting or metallic tabs.

Impactor Design

The impact is induced by a falling mass with a spherical tip. Following the recommendation of many guidelines and standards, the tip has a diameter of 16 mm and is made out of steel, with a load cell being positioned between the tip and the main impactor mass. The falling drop-weight is milled from solid aluminum and has a mass of 2.11 kg. The change in impact energy was achieved through changes in height. After the impact event, two automatically deploying arresting devices prevent secondary damage to the specimen. Figure 5 shows an image of the impact mass resting on these catcher elements.

During the development of the drop-weight tower, an important issue was the adjustment between the guide rods and the impact mass (see Fig. 3). Although extra bearings were initially used, the best and most reliable results were obtained with a well-adjusted clearance in a direct metal-to-metal contact. To verify this approach, potential energy based on height was compared to kinetic energy just prior to impact, calculated from velocity measurements. Only an acceptable level of 2 to 3 % of the set energy was lost, which

can be attributed to frictional losses, nor was any jamming or tilting observed during rebound.

Monitoring Systems

Several measurement and sensor devices were integrated into the setup to observe both the prestressing and the impact event. The approximate location of the sensors can be seen in the Fig. 1.

For measurements of the prestressing process, the cylinder-wise force and displacement measurements of the biaxial texting machine are supplemented my optical strain measurements. For this purpose, a speckle pattern is applied to the underside of the specimens in the unsupported area prior to installation and a Q400 digital image correlation (DIC) system from LIMES, Germany, is set up. The cameras required for the measurements, as well as LED lights for good illumination and contrast, are located under the fixtures, which presents a setup challenge but provides good visual accessibility to the area. The images with the DIC cameras were taken at 1 Hz. Additional data on the prestressing is provided by the biaxial testing machine, which includes measurements of the force and displacement of all four cylinders at a measurement rate of 10 Hz. In addition to load application measurements, the systems were also used to record the unloading process after damage induction.

For the measurements of the impact event, the systems were changed, as much faster sampling rates are required. Two laser distance sensors, a load cell, two high-speed cameras and two acoustic emission sensors were used, the latter being attached to the respective specimens surface in the outer impact area.

Instead of the slower DIC cameras, two high-speed cameras type FASTCAM MINI UX100 manufactured by Photron, Japan, were used, which allowed a recording rate of 8 kHz while maintaining good image resolution. The high-speed cameras not only provide visual information about
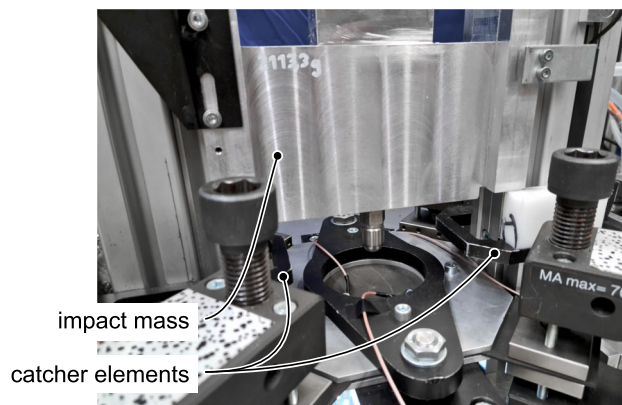
Fig. 5 Image of the impact mass resting on the extended catcher elements

the deflection of the specimen and the damage behavior on its underside, it is also possible to process the image data in the DIC system, allowing areal evaluations of the three-dimensional deformation state.

Two laser measurement systems manufactured by MEL Mikroelektronik, Germany, provide distance data that can also be converted into velocities. A laser sensor of type M7LL/100 is located to the left of the clamping unit and measures the distance to a reflective flag mounted on the left side of the impactor, thus determining its distance and velocity. Recording of the laser sensor signal begins shortly after the impactor passes through a light barrier; this ensures that the M7LL/100 is within range. The second laser sensor, a type M7L/10, measures the deflection of the test specimen under the fixture. The laser is attached to a hinge to allow better optical accessibility for the DIC cameras for strain measurement during load application, while the laser can be reliably moved back into position for the impact event. Since optical measurements are not possible at the laser points location and concentric alignment with the tip of the impactor is difficult to ensure, the laser was positioned slightly offset to the central area with the expected maximum deflection. The M7L/10 laser provides deflection data at a high sampling rate for comparisons, while the camera systems are used for absolute deflection height measurements. This overlap in measurement methods is useful for correlating the data from the drop-weight tower-based systems with the high-speed camera measurements.

The load cell in the impactor is intended for contact history measurement. The load cell is a factory preloaded general purpose ICP quartz force sensor, model 208C05, for pressure measurements up to 22.24 kN, used in conjunction with a battery powered signal conditioner, model 480E09, both manufactured by PCB Piezotronics, USA.

Two high performance iMPact XS acoustic emission and dynamic load sensors, manufactured by iNDTact, Germany, were attached to the specimen to measure breakage events and initiation. The sensors are adhered to the specimens with double-sided adhesive polyester fabric tape prior to testing so that they can be removed and reused after the impact test. The sensors are connected to a 2-channel low-noise broadband charge amplifier type iNDTelect chAMP, also from iNDTact.

The supply and evaluation units of the laser systems as well as the load cell conditioner are connected to a USB-6003 multifunction I/O device from National Instruments (NI), USA, which provides analog-digital data sampling. While one main I/O device controls the electrically actuated pneumatic valves and processes the light barrier and laser data, a second I/O device is used for the load cell's sampling to avoid signal issues likely caused by a ghosting effect. Signal sampling is performed at 50 kHz, and the digital data is sent to a measurement PC for further processing using NI Lab-VIEW, a visual programming language for system design and development that is particularly suited to working with NI hardware devices. Sampling of the acoustic emission sensors is performed by an NI 9223 high-speed analog-to-digital converter, which performs simultaneous sampling at 1 MHz.

Testing Procedure

Performing the test is a multi-step process that provides extensive information about the impact event and the behavior of the composite structure. The steps for testing each specimen on the setup are enumerated below. Prior to the testing, the specimens were primed with white paint, and a speckle pattern was then applied with graphite paint. Care was taken to ensure that these preparations were made in a time frame close to the time of the test.

1. Calibration of high-speed and digital image correlation camera systems.
2. Insertion of the specimen in the support fixture and attachment of the clamping jaws with a specified torque.
3. Mounting of the acoustic emission sensors in the outer areas of the impact zone.
4. Triggering of the automatic movement of the biaxial testing machine until the load on each cylinder is back to zero.
5. Placement of the metal guides and lightly tightening the screw connection, which is done to prevent out-of-plane deflections in the load application areas without causing additional significant frictional forces at the same time.
6. Recording of pre-impact reference pictures with the high-speed camera system.
7. Removal of the deflection laser from the measuring area and start of the recording with the DIC camera system.
8. Application of the preload with holding of the load level for 30 s and subsequent pneumatic clamping the upper frame onto the specimen.
9. Reset of the deflection laser and readying the impact measurement system.
10. Initiation of the impact test with manually mid-point triggering the high-speed camera system and automatic recovery of the falling mass after the impact.
11. Second removal of the deflection laser from the measuring area and start of the recording with the DIC camera system.
12. Unloading of the samples with the subsequent release of the clamped fixture and completion of the DIC camera system measurement.
13. Recording of post-impact reference pictures with the high-speed camera system.
14. Opening of the clamping jaws, resetting of the cylinders of the biaxial testing machine and removal of the specimen.

After the impact test, the data obtained is processed and the sample can be used for investigations of the damage pattern and severity, e.g. by ultrasonic or micrograph analysis.

Data Processing and Evaluation

The sampled digital values of the non-optical measurement system are converted from voltage to the respective units of the measurement system using a LabVIEW script and the calibration values provided by the system manufacturers. Further data analysis is performed using scripts programmed in MATLAB, a multi-paradigm programming language from MathWorks, USA. Figure 6 shows an example of the raw data curves, the processed curves and the determination of comparison values.
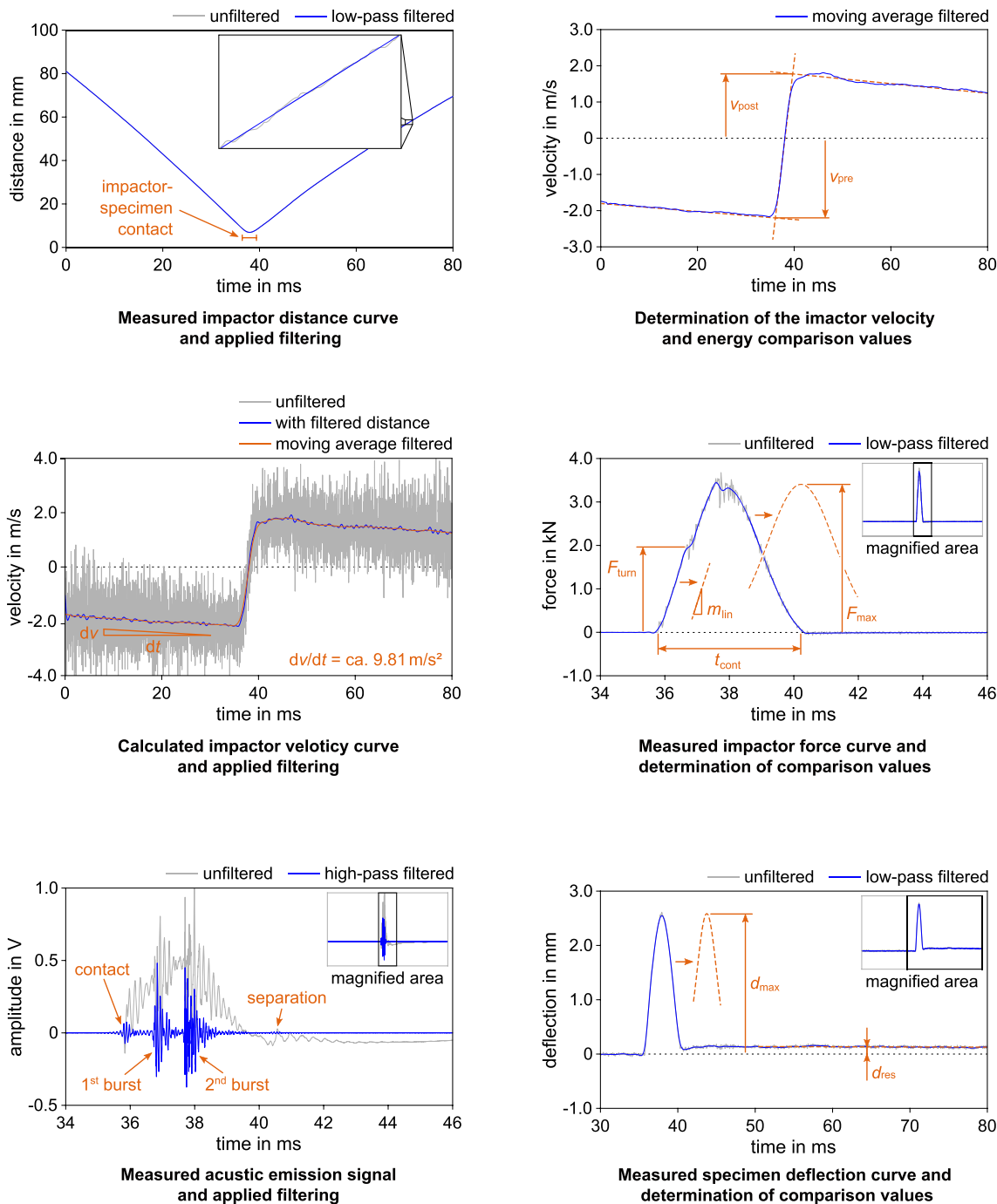
Fig. 6 Data processing of the impact event and specimen behavior data for the non-optical measurement systems

The velocity-time curves of the impactor is calculated based on the discretized distance values of the distance-time curves. Velocity is determined by calculating the difference between a distance measurement point and its predecessor divided by the reciprocal measurement frequency. The application of a filter is necessary for both the displacement-time and velocity-time curves, since this approach leads to irregular value changes. For the displacement-time a minimum-order low-pass filter with a cutoff frequency of 50 Hz, a stop-band attenuation of 60 dB and delay compensation is used. The filtering of the velocity-time curves uses a moving average filter with a window width of 121 values.

For further analysis and comparison of the velocity-time curves, two velocity values in particular are useful. These are the impact velocity shortly before contact and the return velocity afterwards. However, the determination of these values is impeded by a low-frequency oscillation that occurs after impact. Therefore, a linear fitting approach is chosen, where the intersection points indicate the velocity before (v_{pre}) and after (v_{post}) the impact. The difference in the calculated kinetic energies is referred to as dissipated energy and is calculated using

$$E_{diss} = 1/2 \, m \, (v_{pre} - v_{post})^2, \qquad (1)$$

taking into account the mass of the impactor m, which in the present study was set to 2.11 kg.

Further comparative values can be obtained for the impact force and deflection curves using similar curve fitting approaches and a manually tuned automatic determination algorithm. A low-pass filter is used for both types of curves. The same setting of 50 Hz is used for the deflection curves as was used for the distance curves, while the cutoff frequency for the force curves is set to the higher value of 3 kHz. The maximum force (F_{max}) and maximum deflection (d_{max}) are determined with a Gaussian fit using MATLAB's Curve Fitting Toolbox. The fitting is useful to further minimize the effects of any value spikes that may be present in the top region of the peak.

The force curves also provide data on contact time, contact stiffness, and damage initiation. The contact time t_{cont} between impactor and specimen is calculated using the start and end time of the force peak, which is obtained using a force threshold (> 50 Hz). The contact stiffness is estimated by a linear fit in the initial range of the force rise, providing the slope of the fitted function m_{lin} as a comparison value. The linear fit is performed up to a force value where a change in the initial contact slope is observed, which most likely represents the onset of damage or delamination threshold load (DTL). The force value of the turning point F_{turn} is calculated by inverting the derivative of the force curve and finding the most prominent peak, i.e., the region with the lowest slope
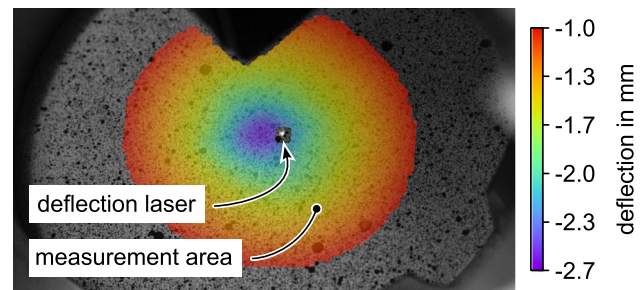
Fig. 7 Exemplary digital image correlation measurement of the specimen deflection with two-high speed cameras. The image shows a compression-tension prestressed specimen shortly before failure (-15 kN/$+15$ kN)

value, between the onset of contact and the maximum force. For the deflection data, a linear fit of the values after the peak is performed to determine the residual deflection d_{res}.

The acoustic emission-time signals were processed with a high-pass filter at 10 kHz, which exhibits similar specifications to the low-pass filter described above. Reduction of the data to selected comparative values is difficult for the emission data. For selected curves, a conversion to the frequency domain with comparison of the burst spectra is planned.

The data processing of the optical measuring systems is done in Istra4D from Dantec Dynamics, Germany. Istra 4D is a software used to control the image correlation measurement system and to analyze the obtained data. To evaluate the image data, it is imported into the software and linked to the previously acquired calibration images. The software then converts the image data using the stored calibration dimensions. In the application, the images may be visualized over time and measurement points may be set. In order to compensate for local fluctuations, most evaluations are carried out in a predefined measuring area, which is automatically transferred to subsequent images. The result is measurement data over time, which allows in-plane and out-of-plane displacements and deformations to be evaluated. Figure 7 shows an exemplary measurement of the specimen deflection shortly before the first visible fractures of the lowest layer occurred.

Feasibility Test

In the following, a first feasibility and applicability test of the described methodology with the test setup and procedure is presented. Specimens impacted under plane mechanical prestress are compared with installed but otherwise unloaded reference specimens. Following the conclusions of Robb et al. [14], a mixed condition with tension and compression appears to be a good basis for comparison. Therefore, a stress state with preloads of -15 kN (compression) on

axis 1 and +15 kN (tension) on axis 2 was selected for the evaluations. See Figure 4 for the axis designation. For the specimens, a quasi-isotropic laminate with a ply structure of $[[+45°/0°/-45°/90°]_2]_s$ was chosen. Test specimens were fabricated from CFRP prepreg type 8552/IM7 manufactured by Hexcel Composites in the United Kingdom. During installation, the 0° alignment of the 2 mm thick specimen was unidirectional to the prestressing axis 1 and +45° aligned between cylinders 1 and 4 or 2 and 3, respectively. The drop height was set to result in an impact energy of 5 J.

Impact Measurements

The processed data from six tests, three for each loading condition, are presented below. These include the displacement and velocity measurements of the impactor, the time history of the impact force, and the history of the deflection measured by a laser on the underside at the center of the specimen. The force and deflection curves are shown in Figs. 8 and 9.

To evaluate the energy and velocity of the impactor, the velocity values pre- and post-impact are compared. The evaluated values are stated as mean values plus/minus the standard deviation of the sample in order to give an estimation on the scattering. The measured pre-impact velocity for both conditions is 2.181 m/s with a deviation of 0.008 m/s for the reference and 0.002 m/s for the preloaded tests. The rebound velocity for the preloaded tests is (1.61 ± 0.08) m/s, which is lower than the reference tests, which yielded (1.82 ± 0.05) m/s. Converted to energy values, the impact energy averages (5.03 ± 0.02) J, with (1.54 ± 0.20) J dissipated in the reference tests and (2.28 ± 0.28) J in the preloaded tests.

Figure 8 shows the moving average filtered (window width of 9) contact force curves. The force curves of the preloaded and reference tests are similar in the initial slope and differ mainly in the upper peak region where a drop in force
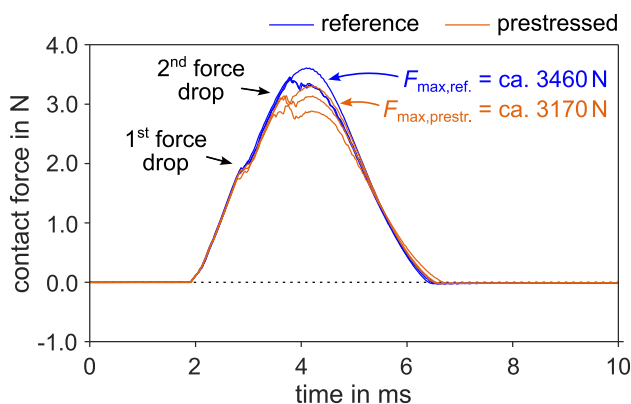
occurs. In comparison, the preloaded tests reach a lower maximum force before the drop, while the reference test reaches higher values. After the drop, the graphs become once again quite similar. One specimen from the reference tests must be excluded from this statement, as no force drop occurred here. Evaluated by the fitting method, the mean impact force for the reference is (3464 ± 98) N compared to (3173 ± 134) N for the preloaded tests. It should be noted that the reference value includes the curve without drop-off, which yielded a force 150 N higher than the other two curves. Without it, the maximum force of the reference curves is 3408 N. The contact stiffness and contact time appears mostly unchanged by the tested stress state.

Figure 9 shows the specimen deflection curves measured with the laser system near the center of impact (see Fig. 7). While the curve progressions are very similar in the beginning, higher deflections are obtained in the preloaded tests than in the reference tests. The values calculated via the fitting method are (2.77 ± 0.04) mm for the preloaded and (2.48 ± 0.11) mm for the reference test. After impact, the laser measurement identifies a residual deformation or specimen displacement of (0.12 ± 0.05) mm for the reference test and (0.50 ± 0.06) mm for the preloaded tests.

Matching with Damage Morphology

One common interpretation of the impact severity of a composite material is the qualitative analysis of intralaminar cracks and delaminations by microscopic investigations. Samples were cut out from the impacted specimens by a water-cooled diamond wheel saw. The samples were embedded in epoxy resin and polished. Light microscopic investigations were performed with an Olympus BX53M microscope. Figure 10 shows the position of the samples and the resulting picture plane for the samples extracted from the impact zone.
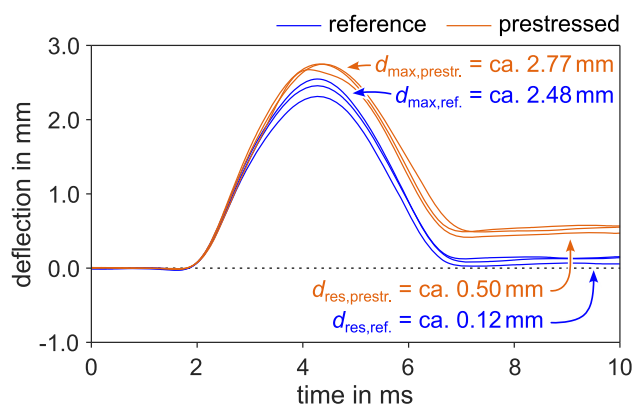

Fig. 8 Comparison of the moving average filtered curves showing the contact force response of impacted CFRP specimens for a non-prestressed reference and a prestressed compression-tension state $(-15 \text{kN}/+15 \text{kN})$

Fig. 9 Comparison of the low-pass filtered curves showing the deflection history of impacted CFRP specimens for a non-prestressed reference and a prestressed compression-tension state $(-15 \text{kN}/+15 \text{kN})$
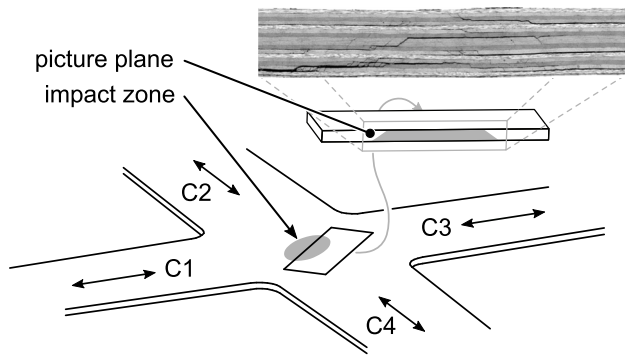
**Fig. 10** Position and picture plane of the samples extracted at the impact zone

Figure 11 shows the light microscopical images of the cross sections of two samples, comparing a sample from the prestressed tests (top) with a sample of the reference tests (bottom). The images were post-processed and adjusted to a uniform level of contrast and brightness. In order to determine the influence of the preload, the observed interlaminar cracks and the delaminations are graphically displayed in sketches beneath the micrographs. On the one hand, it can be seen that with the biaxial mechanical preload the amount and density of interlaminar cracks have increased. On the other hand, no increase in the amount of delaminations was found. Only the length of the delamiation close to the bottom of the cross-section has significantly increased.

Discussion and Conclusions

Based on the available guidelines, standards and scientific studies, a method and setup for testing biaxially prestressed CFRP structures was derived and developed. Cross-shaped specimens are used in the setup, ensuring relatively homogeneous stresses and strains in the mid-impact region for different preloads. In accordance with this design, a round fixation frame and an impact window were chosen. The installation fixture possesses guides to achieve higher compressive loads before stability problems occur. However, alignment of the jaws with the support frame is essential. The design of the impactor is typical, both in terms of mass and diameter of the impactor. However, the tip differs from many of the other biaxial studies presented, where mainly smaller impactor diameters of 12 mm were chosen. The monitoring system and the testing procedure are extensive, but provide comprehensive information on the impact and structural behavior. In order to reduce the many different measurement results to a few comparative values, robust data preparation and automated processing is necessary, which was presented using selected example curves.

Overall, the testing approach and setup seem to work adequately. Nevertheless, specimen mounting and installation is an issue that is frequently raised in impact testing and should be briefly discussed. In the present approach, the size of the circular fixture and impact window is consistent with the shorter projection length of impact windows used in many recommendations. Trial tests conducted alongside the development of the impact tower with rectangular windows (125 mm x 75 mm and 75 mm x 75 mm) as well as with the circular shape of 75 mm diameter allow a basic estimation of the influence of the support type. Compared to the rectangular windows, the circular shape resulted in impacts with slightly higher dissipated energy values and, as subsequent ultrasonic testing revealed, slightly larger dam-
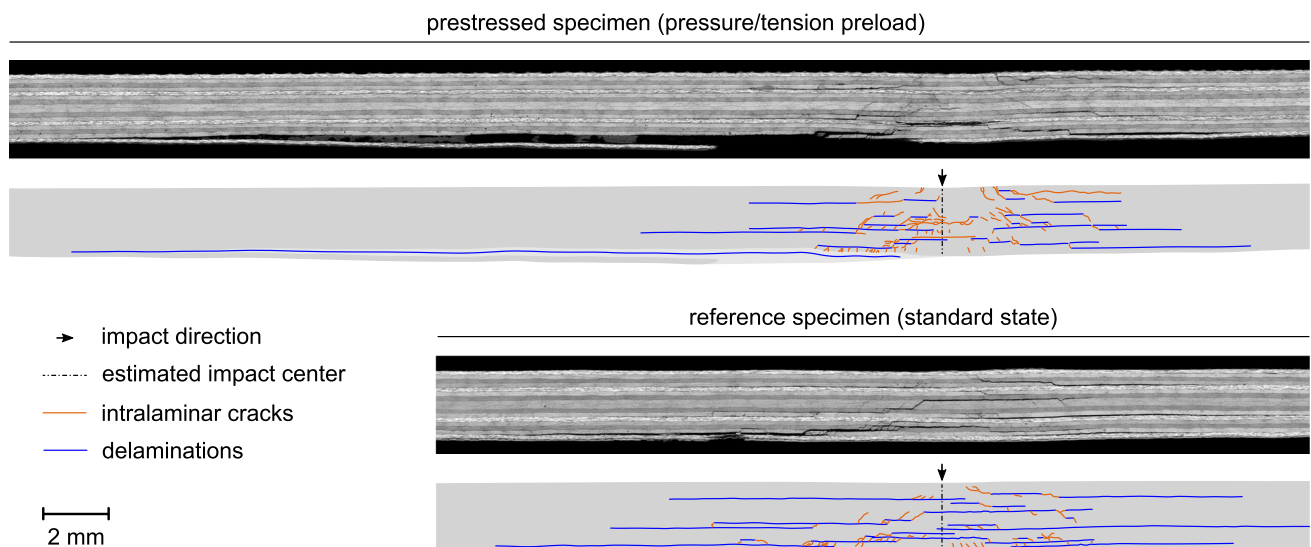
Fig. 11 Light microscopical images of the cross sections of two impacted specimen. Top: Sample of a specimen biaxially preloaded with −15 kN (axis 1) and +15 kN (axis 2). Bottom: Reference specimen without mechanical preloading

age areas, which should be considered when comparing with other research and impact data. It is assumed that the limitation of elastic deformability is the main reason for this behavior. Therefore, direct transfer of the extent of the prestressing effect to other structures is problematic. Rather, the aim is to obtain transferable conclusions and findings on the relevant effects through extensive tests and comparative analyses under identical boundary conditions.

In order to evaluate the test approach and the selected test parameters, an initial feasibility and evaluation test was carried out with prestressed specimens and non-prestressed reference tests. A compressive-tensile condition with a load level of 15 kN was selected as the prestressed condition and 16-ply CFRP structures were damaged. The evaluation focused on the comparison of velocity, energy, force and deflection values. The impact energy during the tests was set to 5 J, which resulted in low-velocity impacts with 2.2 m/s.

In the experiments, differences were found between the impact results of unstressed and prestressed specimens, which only seem attributable to the prestressing state. Interactions, especially involving the fixtures or grips, can be reasonably expected, but there is no evidence of other effects leading to these fairly consistent differences between both test chases. It was found that the compression-tension prestressed structures exhibited a drop in force at a lower force level, higher maximum deflections, significantly larger residual deflections and higher dissipated energy values than the unloaded reference tests. This also showed that the approach to determine the maximum force comparison values with the current Gaussian fit seems to be robust, but does not distinguish between curves with and without force drop-off, which could improve the usefulness of the datasets.

The force and deflection results indicate that the mechanically compression-tension prestressed CFRP specimens responded more sensitively to impact loading, which is in agreement with the increase in dissipated energy values compared to the non-prestressed references. The supplementary light microscopy images also indicate that, at least in the present case study, the prestresses influenced the damage pattern within the specimens. Both the development and occurrence of interlaminar cracks and, to some extent, delaminations seem to be affected.

For the evaluation of the testing approach, the conducted feasibility study can be considered with respect to the cited literature. The results of the experiments appear to be broadly consistent with expectations derived from studies with other materials or experimental setups. For example, the descriptions by Robb et al. [14] of the degrading effect of tension-compression preloads on the investigated panels of chopped-fiber GFRP studied are in line with the findings presented in this paper. In contrast, the contradictory results of Whittingham et al. [15], in which no significant effect of preloads was found, could be explained by the difference in test parameters. The setup presented in this paper is focuses on barely visible impact damage tests, while Whittingham et al. [15] performed impacts with loads close to the penetration level.

Since the present work focused mainly on the methodology, only a small feasibility test was evaluated. To obtain reliable correlations between the prestress state of CFPR structures and the impact behavior, more extensive evaluations with several uniaxial and biaxial prestress configurations are necessary. Additionally, data on the influence of the prestress height and interaction with the impact energy level is desirable for comprehensive conclusions. The goal of this work is to provide information and know-how necessary for a load-dependent design of CFRP primary components to assist in the development of even more efficient and safe composite structures.

Declarations

References

1. Sankar BV, Sun CT (1985) Low-velocity impact response of laminated beams subjected to initial stresses. AIAA J 23(12):1962–1969. https://doi.org/10.2514/3.9203
2. Morlo H, Kunz J (1990) Impact behaviour of loaded composites. Paper presented at the 4th European conference on composite materials, Stuttgart, Germany
3. Nettles AT, Lance DG (1992) Tthe effects of compressive preloads on the compression-after-impact strength of carbon/epoxy. NASA technical paper 3303 available from NASA's technical reports server at https://ntrs.nasa.gov/citations/19930003490

4. Morlo H (1992) Impactverhalten von Verbundwerkstoffen unter dem Einflußäußerer Spannungen. Materials Testing 34(3):74–82. https://doi.org/10.1515/mt-1992-340307

5. Nettles AT, Daniel V, Branscomb C (1995) The effects of tensile preloads on the impact response of carbon/epoxy laminates. Paper presented at the international SAMPE technical conference, Anaheim, CA, USA

6. Chiu S-T, Liou Y-Y, Chang Y-C, Ong C-L (1997) Low velocity impact behavior of prestressed composite laminate. Mater Chem Phys 47:268–272

7. Zhang X, Davies GAO, Hitchings D (1999) Impact damage with compressive preload and post-impact compression of carbon composite plates. Int J Impact Eng 22:485–509

8. Heimbs S, Heller S, Middendorf P, Hähnel F, Weiße J (2009) Low velocity impact on CFRP plates with compressive preload: test and modelling. Int J Impact Eng 36:1182–1193. https://doi.org/10.1016/j.ijimpeng.2009.04.006

9. Pickett AK, Fouinneteau MRC, Middendorf P (2009) Test and modelling of impact on pre-loaded composite panels. Appl Compos Mater 16:225–244. https://doi.org/10.1007/s10443-009-9089-3

10. Choi I-H, Kim I-G, Ahn S-M, Yeom C-H (2010) Analytical and experimental studies on the low-velocity impact response and damage of composite laminates under in-plane loads with structural damping effects. Compos Sci Technol 70:1513–1522. https://doi.org/10.1016/j.compscitech.2010.05.007

11. Toso-Pentecôte N, Johnson AF, Waite S (2012) Experimental study of damage tolerance in pre-stressed composite panels under gas gun impact. Paper presented at the 15th European conference on comoposite materials, Venice, Italy

12. Heimbs S, Bergmann T, Schueler D, Toso-Pentecôte N (2014) High velocity impact on preloaded composite plates. Compos Struct 111:158–168. https://doi.org/10.1016/j.compstruct.2013.12.031

13. Johnson AF, Toso-Pentecôte N, Schueler D (2014) Damage tolerance of pre-stressed composite panels under impact loads. Appl Compos Mater 21. https://doi.org/10.1007/s10443-013-9383-y

14. Robb MD, Arnold WS, Marshall IH (1995) The damage tolerance of grp laminates under biaxial prestress. Compos Struct 32:141–149. https://doi.org/10.1016/0263-8223(95)00077-1

15. Whittingham B, Marshall IH, Mitrevski T, Jones R (2004) The response of composite structures with pre-stress subject to low velocity impact damage. Compos Struct 66:685–698. https://doi.org/10.1016/j.compstruct.2004.06.015

16. Mitrevski T, Marshall IH, Thomson RS, Jones R (2006) Low-velocity impacts on preloaded gfrp specimens with various impactor shapes. Compos Struct 76(3):209–217. https://doi.org/10.1016/j.compstruct.2006.06.033

17. García-Castillo SK, Sánchez-Sáez S, López-Puente J, Barbero E, Navarro C (2007) Impact behaviour of composite panels subjected to in-plane load. Paper presented at the 16th international conference on composite materials, Kyoto, Japan

18. Garnier C, Djilali T, Brault R, Mistou S (2011) Impact resistance of composite materials under biaxial preloading. Key Eng Mater 482:39–48. https://doi.org/10.4028/www.scientific.net/KEM.482.39

19. Kurşun A, Şenel M (2011) Investigation of the effect of low-velocity impact on composite plates with preloading. Exp Tech 37(6):41–48. https://doi.org/10.1111/j.1747-1567.2011.00738.x

20. Kurşun A, Şenel M, Enginsoy HM (2015) Experimental and numerical analysis of low velocity impact on a preloaded composite plate. Adv Eng Softw 90:41–52. https://doi.org/10.1016/j.advengsoft.2015.06.010

21. Gerke S, Adulyasak P, Brünig M (2017) New biaxially loaded specimens for the analysis of damage and fracture in sheet metals. Int J Solids Struct 110–111:209–218. https://doi.org/10.1016/j.ijsolstr.2017.01.027

22. Brünig M, Gerke S, Zistl M (2020) Experiments on damage and fracture mechanisms in ductile metals under non-proportional loading paths. In: Altenbach H, Brünig M, Kowalewski ZL (eds) Plasticity, damage and fracture in advanced materials, advanced structured materials. Springer, Cham, Germany, pp 19–33